Journal of Power Sources 209 (2012) 158–162

Contents lists available at SciVerse ScienceDirect

Journal of Power Sources

journal homepage: www.elsevier.com/locate/jpowsour

Short communication

Oxygen adsorption on the $Ag/La_{1-x}Sr_xMnO_3(0\,0\,1)$ catalysts surfaces: A first-principles study

Yongjun Zhou[a,b], Zhe Lü[a,*], Bo Wei[a], Xingbao Zhu[a], Xiqiang Huang[a], Wei Jiang[a], Wenhui Su[a]

[a] Center for the Condensed Matter Science and Technology, Department of Physics, Harbin Institute of Technology, Harbin 150001, China
[b] College of natural sciences, Shenyang Aerospace University, Shenyang 110034, China

ARTICLE INFO

Article history:
Received 10 January 2012
Received in revised form 22 February 2012
Accepted 23 February 2012
Available online 3 March 2012

Keywords:
First-principles calculations
Oxygen adsorption
Ag catalytic
Solid oxide fuel cells

ABSTRACT

The oxygen adsorption on Ag/LSM(0 0 1) catalysts surfaces has been investigated using first-principles density functional theory calculations. The most favorable oxygen adsorption sites are found to be atop surface Mn atoms on the MnO_2-terminated surface and on the hollow positions of the La(Sr)O-terminated LSM(0 0 1) surface. The calculated adsorption energies for Ag atom demonstrate that the Ag adsorption at O site is much more favorable than Mn site. The atomic relaxation results indicate that Ag doping produces a strong local perturbation and a large effect on the surface properties. No significant improvement for oxygen adsorption is found due to Ag doping. However, the O_2 adsorption energy increases from 0.495 eV to 0.937 eV due to the pre-adsorbed Ag. It is pre-adsorbed Ag that facilitates O_2 adsorption on surface. The bond length and bond population of O_2 molecule indicate that Ag atom facilitates O_2 molecule dissociative adsorption. The adsorbed Ag on LSM strengthens its activity as SOFCs cathode by acting as an active center at the surface.

1. Introduction

Solid oxide fuel cells (SOFCs) have attracted considerable attention due to their high energy conversion efficiency and excellent fuel flexibility [1–4]. Sr-doped $LaMnO_3$ ($La_{1-x}Sr_xMnO_3$, hereafter denoted as LSM) is one of the extensively studied perovskite-type cathode materials for SOFCs due to its excellent electrocatalytic activity for the oxygen reduction reaction at high temperatures, good electronic conductivity, and chemical stability at operating conditions [5–7]. Nevertheless, the high operating temperature (800–1000 °C) causes some problems (i.e. high cost; enhanced aging, etc.). Lowering the operating temperature, however, decreases the power density of SOFCs due to decreasing catalytic activity. To make SOFCs economically competitive, the development of optimal cathode materials with high catalytic activity at lower temperatures (i.e. 500–800°C) has been an active research topic. One way to overcome this limitation may be to increase catalytic activity of the cathode for oxygen reduction and improve the performance of the cathode by adding noble metals (Ag, Pd, Pt) to the cathode. Silver is a potential component for the cathode in SOFCs operated at less than 800 °C due to its good catalytic activity, high electrical conductivity and relatively low cost [8]. According to recent experiments [9–12], Ag/LSM system has also been reported to be a prominent catalyst for the oxygen reduction reaction in SOFCs applications.

The cathodic reaction comprises the adsorption of oxygen molecule on the surface, followed by surface or bulk diffusion toward the electrolyte, charges transfer and ion incorporation into the electrolyte. Recently, density functional theory (DFT) study method [13–16] has proved to be a powerful tool to elucidate reaction mechanism as the technique can provide electronic structure, geometrical parameters and adsorbed intermediate species. Branda et al. [17] and Tang et al. [18] investigated the properties of Ag adsorbed on the $CeO_2(1\,1\,1)$ surface by DFT method. Similarly, Wang et al. [19] systematically examined the reduction processes of oxygen molecule adsorbed on the Ag/CeO_2 surface, implying that oxygen molecules prefer being reduced at triple-phase boundary (TPB).

However, the Ag/LSM system is less studied compared with the cases of Ag/CeO_2. No theoretical investigation so far has been carried out about the oxygen adsorption on Ag/LSM(0 0 1) catalysts surfaces in the literature. Elucidating the mechanisms of oxygen reduction on Ag/LSM(0 0 1) catalysts surfaces is beneficial for understanding the limitations of the currently used materials in SOFCs technology and aiding the development of higher performance materials.

In the present paper, we report the oxygen adsorption mechanisms on Ag/LSM(0 0 1) catalyst surfaces using first-principles calculations based on DFT and pseudopotential method. First, adsorption properties for O_2 molecule on both MnO_2-LSM(0 0 1)

* Corresponding author. Tel.: +86 451 86418420; fax: +86 451 86418420.
E-mail address: lvzhe@hit.edu.cn (Z. Lü).

0378-7753/$ – see front matter © 2012 Elsevier B.V. All rights reserved.
doi:10.1016/j.jpowsour.2012.02.097

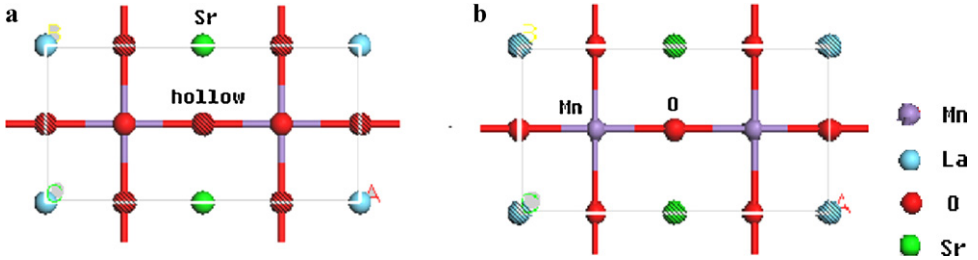

Fig. 1. Schematic top view of oxygen possible adsorption sites: the La(Sr)O-terminated LSM(0 0 1) surface (a) and the MnO_2-terminated LSM(0 0 1) surface (b). Hatched denote atoms in the subsurface plane.

and La(Sr)O-LSM(0 0 1) terminal surface are extensively investigated. Second, the electronic properties of interaction between Ag atom and MnO_2-terminated surface are calculated. Finally, a comparison study of the oxygen adsorption mechanisms for pre-adsorbed and doped Ag on MnO_2-terminated surface is carried out, which provides a new direction for improving electrocatalysis.

2. Computational method

We carry out first-principles calculation using CASTEP code [20], which uses the plane-wave pseudopotential total energy calculation method based on the DFT. The interaction between nuclei and electrons is approximated with Vanderbilt ultra-soft pseudopotential [21] and the Wang and Perdew [19,22] parametrization is taken as the exchange-correlation functional in the generalized-gradient approximation. After test calculation, kinetic energy cutoff at 420 eV and the Brillouin zone sampling $2 \times 3 \times 1$ Monkhorst–Pack [23] *k*-points for surface is adopted. By further increasing the kinetic energy cutoff and the number of *k*-points the change in the results could be neglected. La, Mn, Sr, O, Ag atoms are described by $11(5s^2 5p^6 5d^1 6s^2)$, $7(3d^5 4s^2)$, $10(4s^2 4p^6 5s^2)$, $6(2s^2 2p^4)$, $11(4d^{10} 5s^1)$ valence electrons, respectively. A relaxation is performed for the constructed supercell by using Broyden–Fletcher–Goldfarb–Shanno algorithm [24] to minimize the energy with respect to atomic position. In calculations the tolerances for self-consistence are set at 1.0×10^{-6} eV atom^{-1} for total energy, 0.05 eV Å^{-1} for force, 2.0×10^{-5} eV atom^{-1} for band energy, 0.1 GPa for maximum stress and 0.002 Å for the maximum displacement. We chose the spin-polarized method to properly describe the magnetic property of LSM and the triplet ground state of oxygen [25–27]. Under SOFCs operation conditions $LaMnO_3$(LMO) is paramagnetic ($T_N = 140$ K). We perform all calculations for the ferromagnetic (FM) configuration because FM configuration of LSM is more stable than the anti-ferromagnetic (AFM) configuration [14].

According to Hund's rule, the lowest energy corresponds to the maximal spin projection on the Mn^{3+} ion ($S_z = 2$, four spin-up d electrons occupy t_{2g} and e_g levels). In this study, we consider cubic perovskite structure of pm3 m since the LMO-based cathode materials has a cubic structure under SOFCs operating conditions [28,29]. We calculate cubic phase of LSM-based crystals doped with Sr, substituting for La atoms. Fig. 1 shows a schematic top view of possible oxygen adsorption sites on the La(Sr)O-LSM(0 0 1) slab with Sr dopant at $x = 0.16$ in the surface plane (a) and on the MnO_2-LSM(0 0 1) slab with Sr dopant in the subsurface plane (b). In SOFCs applications, LMO is usually doped 10–20% of Sr substituting for La [30].

We model the O_2 adsorption on a much less polar LSM(0 0 1) surface with respect to LSM(1 1 0) surface consisting of alternating MnO_2/La(Sr)O plane. We find in particular that 6- and 7-plane slabs are thick enough and show main property convergence. The periodically repeated slabs are separated by a large vacuum gap of 15 Å, in order to prevent an interaction between the two surfaces through the vacuum region. In the geometric optimization, only the top 3 layers are allowed to be relaxed (Fig. 2).

The adsorption energy is calculated according to $E_{ads} = E_{[O2]} + E_{[surface]} - E_{[O2/surface]}$, where $E_{[O2/surface]}$ and $E_{[surface]}$ are the calculated electronic energies of bonded oxygen species on the surface and a clean surface, respectively, and $E_{[O2]}$ denotes the energy for triplet O_2. The adsorption energy is a criterion to determine the stability of the adsorption.

3. Results and discussion

3.1. O_2 molecule adsorbed on the LSM(0 0 1) surfaces

The bulk calculations are initially performed and compared with previous calculations [31] and experimental value [32,33] to confirm that the applied parameters give confident results (Table 1). As can be seen from the calculated adsorption properties in Table 2, the O_2 adsorption energies for Mn site on the MnO_2-terminated surface is 0.495 eV and for hollow site on the La(Sr)O-terminated surface is 0.709 eV. It can be confirmed that the most favorable oxygen adsorption sites are found to be atop surface Mn atoms on the MnO_2-terminated surface and on the hollow positions of the La(Sr)O-terminated LSM(0 0 1) surface. The Mulliken charges of O_2 molecule are −0.20 at Mn site, while it is −0.42 at hollow site. The O_1–O_2 bond length is largely stretched (O_1–O_2 distance of 1.302 Å,

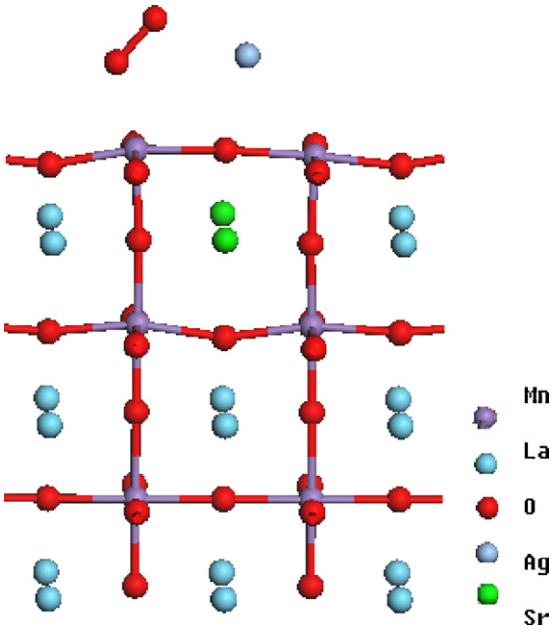

Fig. 2. The optimized structure of the O_2 adsorption on Ag pre-adsorbed LSM(0 0 1) surface.

Table 1
The optimized lattice constant of bulk $LaMnO_3$ and $SrMnO_3$.

	Lattice constant (Å)			
	WIEN-2k [31]	CRYSTAL-03	Experiment	This work
$LaMnO_3$	3.921	3.967	3.947[a]	3.978
$SrMnO_3$	3.848	3.840	3.806[b]	3.894

[a] Experimental data from Ref. [32].
[b] Experimental data from Ref. [33].

compared to the calculated equilibrium gas phase value of 1.238 Å which is slightly larger than experimental value of 1.210Å [34]) at the hollow position of the La(Sr)O-terminated LSM(0 0 1) surface. The adsorbed molecule could be considered as a kind of the superoxo-radical (hydrogen superoxide radical HO_2 1.33 Å [14]). At the same time, the bond population of O_1–O_2 decreases to 0.34 at hollow site. Both the bond length and the bond population indicate that the adsorption of O_2 molecule on hollow position of the La(Sr)O-terminated surface is readily dissociated. The bond population of O_1–M_{surf} at O site is −0.01, meaning a non-covalent interaction between O_2 molecule and surface ion. For other adsorption sites, the bond population are positive, which indicates the covalent bonds are formed between O_2 molecule and surface ion.

3.2. Main electronic properties for Ag adsorption and doping on LSM(0 0 1) surface

The Ag adsorption properties are investigated and the results are listed in Table 3. We consider two different sites on MnO_2-terminated surface (Fig. 1b): Mn site and O site. Because the surface is attractive for the oxygen incorporation process due to smaller oxygen vacancy formation energy [7]. We find that Ag adsorption at O site is much more favorable (E_{ad} = 2.091 eV) than Mn site (E_{ad} = 1.736 eV), which are similar to the value of Ag adsorbed on CeO_2(1 1 1) surface [17]. The effective charges of the structure are obtained by Mulliken charges analysis. The Mulliken charges of Ag are 0.11 at O site, while this number is reduced to 0.05 at Mn site. Compared to pure surface, the Ag adsorption introduces charge transfer, especially the charges of Mn atom in the topmost plane decrease from 0.86 to 0.64, 0.76, respectively. The bond populations of Ag–Mn_s and Ag–O_s reach 0.29 and 0.12, which demonstrate that covalent bonds between Ag and surface ion are formed.

Due to the very close ionic radii of Ag^+ (0.126 nm), La^{3+} (0.106 nm) and Sr^{2+} (0.113 nm) [11], a certain amount of the Ag^+ doped onto the LSM(0 0 1) surface could partially replace La^{3+} and Sr^{2+}, and occupy the A-sites in the perovskite lattice, as reported by some experiments [35–37]. We construct doped Ag in the subsurface plane based on the pure LMO(0 0 1) surface model. The introduction of Ag ions substituting for La ions in the second plane produces a strong local perturbation. The dopant Ag atom relaxes toward the surface, forming the vacancy and interstitial Ag. In order to compare the calculated surface structure, the amplitudes of surface rumpling defined as the relative displacement of O atoms with respect to Mn atoms in the surface layer [38]. Analysis of surface relaxation shows a considerable rumpling (s = 0.236, approximately 5.9% of a_0) compared to the pure LMO (s = 0.178 is in agreement with the literature [39], which could be checked by means of LEED experiments) surface structure. O ions of the MnO_2-terminated surface strongly move outward (0.159 Å), while surface Mn ions move inward (0.077 Å) toward the slab center. On the MnO_2-terminated surfaces both O and Mn ions become additionally more positive by 0.04 and 0.08, respectively. These indicate that the doping of Ag has very large effect on the surface properties.

3.3. The catalytic effect of Ag in the O_2 adsorption of LSM(0 0 1) surface

For the doping, the O_2 adsorption energy at Mn site is calculated with respect to Ag substituting for La in the second plane. The value is 0.102 eV, much smaller than the adsorption on pure LMO surface (E_{ad} = 0.298 eV) and LSM surface (E_{ad} = 0.495 eV). The increased O_2 molecule bond population (0.42 vs. 0.40 for LMO) and relatively long distance of O_{ads}–Mn_s (2.094 Å vs. 2.000 Å for LMO) also indicate that no significant improvement for oxygen adsorption is found due to Ag doping.

For pre-adsorbed Ag, the catalytic effect for O_2 adsorption on MnO_2-terminated surface is investigated. We construct a surface model with O_2 molecule adsorbed Mn site and Ag atom adsorbed O site and simulate three-phase boundary area for oxygen reduction reaction (Fig. 2). The adsorption energy dramatically increases from 0.495 eV to 0.937 eV due to pre-adsorbed Ag. It is pre-adsorbed Ag that facilitates O_2 adsorption.

As can be seen from Table 4, an important consequence of adsorption at the interface is that the bond length of O_2 molecule increases from 1.270 Å to 1.370 Å and the bond population of O_1–O_2

Table 2
Calculated adsorption properties for O_2 molecule on LSM (0 0 1) surface.

Ads. site	E_{ads} (eV)	Distance (Å)		Charges		Bond population	
		O_1–O_2 [a]	O_1–M_{surf} [b]	O_1	O_2	O_1–M_{surf}	O_1–O_2
MnO_2-LSM(0 0 1)							
O	0.072	1.242	2.982	0.00	−0.04	−0.01	0.40
Mn	0.495	1.270	2.000	−0.12	−0.08	0.11	0.42
La(Sr)O-LSM(0 0 1)							
Sr	0.584	1.274	2.443	−0.23	−0.06	0.21	0.37
Hollow	0.709	1.302	2.595	−0.28	−0.14	0.26	0.34

[a] O_1 atom nearest to the surface, O_2 atom far to the surface.
[b] O_1–M_{surf} correspond to the distance between O_1 and the nearest surface atoms.

Table 3
Calculated adsorption properties for Ag atom on LSM (0 0 1) surface.

Ads. site	E_{ads} (eV)	Distance (Å)		Charges			Bond population	
		Ag–O_s [a]	Ag–Mn_s	Ag	O_s	Mn_s	Ag–O_s	Ag–Mn_s
Mn	1.736	3.381	2.667	0.05	−0.70	0.64	–	0.29
O	2.091	2.228	2.957	0.11	−0.74	0.76	0.12	0.06

[a] O_s atom on the surface, Mn_s atom on the surface.

Table 4
Comparative O_2 adsorption properties on LSM(0 0 1) surface with and without Ag pre-adsorbed.

	E_{ads} (eV)	Distance (Å)		Charges				Bond population	
		O_1–O_2	O_1–Mn_s	O_1	O_2	Mn_s	Ag	O_1–O_2	O_1–Mn_s
No Ag pre-adsorbed	0.495	1.270	2.000	−0.12	−0.08	0.92/0.87	–	0.42	0.11
Ag pre-adsorbed	0.937	1.370	2.045	−0.17	−0.24	0.89/0.76	0.51	0.37	0.21

Table 5
Calculated O atom adsorption properties on Ag/MnO_2-terminated surface.

Ads. site	E_{ads} (eV)	Distance (Å)		Charges			Bond population	
		O–Mn_s	O–Ag	O	Mn_s	Ag	O–Mn_s	O–Ag
Mn	0.934	1.749	2.193	−0.49	0.82	0.42	0.52	0.26
Hollow	0.475	–	2.006	−0.62	0.81	0.54	–	0.81

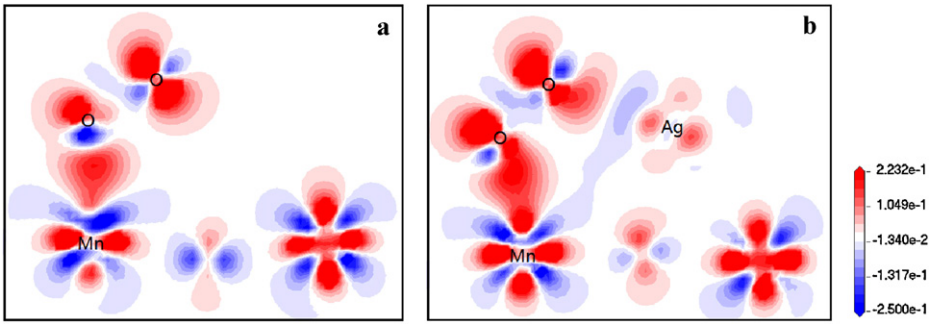

Fig. 3. Difference electron density maps highlighting the electron charge density redistribution due to the Ag pre-adsorption for the (a) without Ag adsorption and (b) with Ag adsorption. Red and blue colors have been used to represent accumulation and depletion of charge, respectively. (For interpretation of the references to color in this figure legend, the reader is referred to the web version of the article.)

decreases from 0.42 to 0.37, which demonstrate that pre-adsorbed Ag atom facilitates O_2 molecule dissociate to O atoms, thus contributing to the surface oxygen diffusion process. The charges of O_2 molecule increase from 0.20 to 0.41 and the bond population of O_1–Mn_s increases from 0.11 to 0.21, implying that ionic bond and covalent bond of adsorption molecule and surface ions become strong apparently. The Mulliken population analysis results are nicely supported by the change of electron density. The different charge density is constructed by subtracting the electronic densities of O_2/LSM(0 0 1) from the densities of an O_2 molecule and a clean LSM(0 0 1) for Fig. 3(a) and by subtracting the electronic densities of O_2/Ag/LSM(0 0 1) from the densities of an O_2 molecule and a clean Ag/LSM(0 0 1) for Fig. 3(b). In this way, the presentation highlights the charge rearrangement upon bond formation and more obvious electron density accumulation in the O–Mn bonding regions compared to without pre-adsorbed Ag. So the silver is highly active for adsorption and dissociation of oxygen species. This may strengthen LSM substrate activity due to pre-adsorbed Ag and active center is formed in surface, which enhances the electrocatalytic activity of LSM as SOFCs cathode materials at low temperature.

Along with the O_2 molecule adsorption, the adsorption properties for O atom on Ag/LSM(0 0 1) surface are calculated. Table 5 shows a strong preference for O atom adsorption over the Ag/LSM(0 0 1) surface Mn ion, which is in agreement with the pure LSM(0 0 1) surface [15,40]. The bond population indicates that stronger covalent bond is formed between O atom and Ag atom. The electron charges of 0.49 are transferred to the adsorbed O atom from nearest ions, while this number is increased to 0.62 at hollow site.

4. Conclusions

First-principles calculations based on DFT with pseudopotential method have been used to oxygen adsorption on the Ag/LSM(0 0 1) catalysts surface. The obtained results are given as follows:

(1) The most favorable oxygen adsorption sites are found to be atop surface Mn atoms on the MnO_2-terminated surface and on the hollow positions of the La(Sr)O-terminated LSM(0 0 1) surface.
(2) The calculated electronic properties of interaction between Ag atom and surface demonstrate that the Ag adsorption energies at Mn, O sites are 1.736 and 2.091 eV, respectively. The Ag adsorption at O site is much more favorable than Mn site. The atomic relaxation results indicate that Ag doped in the second plane produces a strong local perturbation and a large effect on the surface properties.
(3) No significant improvement for oxygen adsorption is found due to Ag doping. However, the O_2 adsorption energy increases from 0.495 eV to 0.937 eV due to pre-adsorbed Ag. It is pre-adsorbed Ag that facilitates O_2 adsorption. The calculated bond length and bond population of O_2 molecule indicate that Ag atom facilitates O_2 molecule dissociate to O atoms. The adsorbed Ag on LSM strengthens its activity as SOFCs cathode by acting as an active center at the surface.

Acknowledgments

The authors gratefully acknowledge the Projects (50902032, 20901020) supported by National Natural Scientific Foundation

of China. The authors also acknowledge the support of High-performance Computing Center, Harbin Institute of Technology.

References

[1] Y.M. Choi, D.S. Mebane, M.C. Lin, M. Liu, Chem. Mater. 19 (2007) 1690.
[2] M. Koyama, M. Kubo, A. Miyamoto, Appl. Surf. Sci. 244 (2005) 598.
[3] W. An, D. Gatewood, B. Dunlap, C.H. Turner, J. Power Sources 196 (2011) 4724.
[4] T. Jin, K. Lu, J. Power Sources 197 (2012) 20.
[5] S.B. Adler, Chem. Rev. 104 (2004) 4791.
[6] Y. Choi, D. Mebane, J.H. Wang, M. Liu, Top. Catal. 46 (2007) 386.
[7] S. Piskunov, T. Jacob, E. Spohr, Phys. Rev. B 83 (2011) 073402.
[8] C. Sun, R. Hui, J. Roller, J. Solid State Electronchem. 14 (2010) 1125.
[9] V.A.C. Haanappel, D. Rutenbeck, A. Mai, S. Uhlenbruck, D. Sebold, H. Wesemeyer, B. Rowekamp, C. Tropartz, F. Tietz, J. Power Sources 130 (2004) 119.
[10] S. Uhlenbruck, F. Tietz, V. Haanappel, D. Sebold, J. Solid State Electronchem. 8 (2004) 923.
[11] W. Wang, H. Zhang, G. Lin, Z. Xiong, Appl. Catal. B 24 (2000) 219.
[12] W. Zhou, Z. Shao, F. Liang, Z.G. Chen, J. Mater. Chem. 21 (2011) 15343.
[13] Y.M. Choi, M.E. Lynch, M.C. Lin, M. Liu, J. Phys. Chem. C 113 (2009) 7290.
[14] Y.A. Mastrikov, R. Merkle, E. Heifets, E.A. Kotomin, J. Maier, J. Phys. Chem. C 114 (2010) 3017.
[15] E.A. Kotomin, Y.A. Mastrikov, E. Heifets, J. Maier, Phys. Chem. Chem. Phys 10 (2008) 4644.
[16] Y.M. Choi, M.C. Lin, M.L. Liu, J. Power Sources 195 (2010) 1441.
[17] M. Branda, N.C. Hernandez, J.F. Sanz, F. Illas, J. Phys. Chem. C 114 (2010) 1934.
[18] Y. Tang, H. Zhang, L. Cui, C. Ouyang, S. Shi, W. Tang, H. Li, L. Chen, J. Power Sources 197 (2012) 28.
[19] J.H. Wang, M. Liu, M.C. Lin, Solid State Ionics 177 (2006) 939.
[20] S.J. Clark, M.D. Segall, C.J. Pickard, P.J. Hasnip, M.J. Probert, K. Refson, M.C. Payne, Z. Kristallogr. 220 (2005) 567.
[21] D. Vanderbilt, Phys. Rev. B 41 (1990) 7892.
[22] J.P. Perdew, J.A. Chevary, S.H. Vosko, K.A. Jackson, M.R. Pederson, D.J. Singh, C. Fiolhais, Phys. Rev. B 46 (1992) 6671.
[23] H.J. Monkhorst, J.D. Pack, Phys. Rev. B 13 (1976) 5188.
[24] B.G. Pfrommer, M. Cote, S.G. Louie, M.L. Cohen, J. Comput. Phys. 131 (1997) 233.
[25] Y.M. Choi, M.C. Lin, M. Liu, Angew. Chem. 119 (2007) 7352.
[26] G. Pilania, R. Ramprassad, Surf. Sci. 604 (2010) 1889.
[27] Y.A. Mastrikov, E. Heifets, E.A. Kotomin, J. Maier, Surf. Sci. 603 (2009) 326.
[28] R.A. Evarestov, E.A. Kotomin, E. Heifets, J. Maier, G. Borstel, Solid State Commun. 127 (2003) 367.
[29] R.A. Evarestov, E.A. Kotomin, Y.A. Mastrikov, D. Gryaznov, E. Heifets, J. Maier, J. Phys. Rev. B 72 (2005) 214411.
[30] D. Fuks, S. Dorfman, J. Felsteiner, L. Bakaleinikov, Solid State Ionics 173 (2004) 107.
[31] D. Fuks, L. Bakaleinikov, E. Kotomin, J. Felsteiner, Solid State Ionics 177 (2006) 217.
[32] J.R. Carvajal, M. Hennion, F. Moussa, A.H. Moudden, Phys. Rev. B 57 (1998) R3190.
[33] M. Towler, N. Allan, N. Harrison, V. Saunders, Phys. Rev. B 50 (1994) 5041.
[34] D.R. Lide (Ed.), CRC Handbook of Chemistry and Physics, CRC Press, Boca Raton, FL, 1993.
[35] T. Tang, K. Gu, Q. Cao, D. Wang, J. Mag. Mag. Mater. 222 (2000) 110.
[36] K. Song, H. Cui, S. Kim, S. Kang, Catal. Today 47 (1999) 155.
[37] V. Choudhary, B. Uphade, S. Pataskar, Fuel 78 (1999) 919.
[38] W. Shi, S. Xiong, Surf. Sci. 604 (2010) 1987.
[39] Y.A. Mastrikov, E.A. Kotomin, E. Heifets, J. Maier, Condes. Matter (2008), arXiv:0807.1864v1.
[40] Y. Lee, J. Kleis, J. Rossmeisl, D. Morgan, Phys. Rev. B 80 (2009) 224101.